J.C.S. Faraday II, 1980, 76, 1147–1160

Power Reflection Spectroscopy near the Brewster Angle

Molecular Dynamics of Liquids

BY MYRON EVANS

Chemistry Department, The University College of Wales, Aberystwyth SY23 1NE

Received 11*th September*, 1979

Power reflection spectroscopy has been investigated theoretically for potential use with dipolar liquids as a means of evaluating the molecular dynamics and interactions. Calculations have been made with and without a dynamic internal field correction. This does not affect in any way the major features of the spectra in σ and π polarisation at various values of ϕ, the incident angle. Near a Brewster angle ($\phi_B = \tan^{-1} \varepsilon_p^{\frac{1}{2}}$, where ε_p is the high frequency permittivity), the reflectivity r develops a high frequency peak, typically in the mid-infrared. This brings the study of librational molecular dynamics within range of conventional spectrometers, provided that the problems of amplification and detection of the reflected r_π radiation can be overcome.

In principle, reflection spectroscopy provides us with information simultaneously both about the real and imaginary parts of the complex refractive index $n^* = \varepsilon^{*\frac{1}{2}}$, where ε^* is the (complex) dielectric permittivity of the surface under investigation. However, the fundamental equations of reflection spectroscopy are complicated and for this reason the absorption technique tends to be used almost exclusively, for example in the infrared. The computers available now remove this disadvantage. It is the purpose of this paper to show that measurements of the reflectivity (R) in the far- and mid-infrared is an additional useful source of molecular dynamical information which has as yet remained untapped. If we define by ε_0 the real part of ε^* at static frequencies and by ε_p that at frequencies just past the f.i.r. Poley absorption,[1] then polarised reflectivity measurements very near the incident Brewster angle $\phi_B = \tan^{-1} \varepsilon_p^{\frac{1}{2}}$ are particularly rewarding; below we explain why. Effectively, our calculations show that the Debye and Poley features in ε^* of dipolar liquids are shifted to much higher frequencies using ϕ_B in r_π polarisation,[2] thus bringing the former within range of the f.i.r. Michelson inteferometer [3] and shifting the latter up into the mid-infrared ($\approx$ 200-1000 cm^{-1}), bringing it within range of conventional grating spectrometers and making its measurement a routine matter given sufficiently sensitive signal amplification. The paper is developed as follows. First, we specify our reflectivity equation. Secondly, a brief description is given of the molecular dynamical models used and the internal dynamical-field correction. We use linearised Mori 3 variable theory for the orientational autocorrelation function $\langle \boldsymbol{\mu}(t) \cdot \boldsymbol{\mu}(0) \rangle$, where $\boldsymbol{\mu}$ is the molecular dipole moment. This model has been extensively tested by Evans *et al.*[4] and has been adopted by Lobo *et al.*[5] to incorporate the idea of dielectric friction introduced by Nee and Zwanzig [6] and Scaife.[7] This is the "dynamical equivalent" of the Onsager reaction field. Finally, we illustrate some theoretical spectra at various incident angles, ϕ, (normal, Brewster and glancing) and discuss the implications.

FUNDAMENTAL EQUATIONS OF POWER REFLECTION SPECTROSCOPY

These are discussed fully by Brugel [2] for infrared spectroscopy and in many fundamental texts. However, we reproduce some here for convenience. Define the reflective power $R(\bar{\nu})$ as the ratio of the energy reflected to that incident. Here $\bar{\nu}$ is the wavenumber in cm^{-1}. The direction of vibration of the radiation is taken with respect to the plane of incidence. The component vibrating parallel to this plane is denoted by π and that perpendicular by σ. The reflective powers r_π and r_σ are then given by Fresnel's formulae and Snell's law, so that with polarised radiation:

$$r_\sigma = \frac{\sin^2(\phi-\chi)}{\sin^2(\phi+\chi)}; \quad r_\pi = \frac{\tan^2(\phi-\chi)}{\tan^2(\phi+\chi)}; \quad \sin\phi = n^* \sin\chi.$$

Writing

$$n^* = n(1-i\kappa) \tag{1}$$

it follows that

$$r_\sigma = \frac{a^2+b^2-2a\cos\phi+\cos^2\phi}{a^2+b^2+2a\cos\phi+\cos^2\phi}; \tag{2}$$

$$r_\pi = r_\sigma \frac{a^2+b^2-2a\sin\phi\tan\phi+\sin^2\phi\tan^2\phi}{a^2+b^2+2a\sin\phi\tan\phi+\sin^2\phi\tan^2\phi}; \tag{3}$$

where

$$a = \{\tfrac{1}{2}[n^2(1-\kappa^2)-\sin^2\phi]+\tfrac{1}{2}[(n^2(1-\kappa^2)-\sin^2\phi)^2+4n^4\kappa^2]^{\frac{1}{2}}\}^{\frac{1}{2}};$$

$$a^2+b^2 = \frac{\tfrac{1}{2}[n^2(1-\kappa^2)-\sin^2\phi]+\tfrac{1}{2}[(n^2(1-\kappa^2)-\sin^2\phi)^2+4n^4\kappa^2]^{\frac{1}{2}}+2n^4\kappa^2}{n^2(1-\kappa^2)-\sin^2\phi+\{[n^2(1-\kappa^2)-\sin^2\phi]^2+4n^4\kappa^2\}^{\frac{1}{2}}}.$$

The complexity of these relations is no obstacle using a convenient microprocessor or main frame system. The σ and the π polarised reflectivities may now be related to the molecular dipole autocorrelation function $\langle \boldsymbol{\mu}(t)\cdot\boldsymbol{\mu}(0)\rangle$ through the link

$$\varepsilon^* \equiv (\varepsilon'-i\varepsilon'') = [n(1-i\kappa)]^2. \tag{4}$$

Here ε' and ε'' are the dielectric permittivity and loss, related to the infrared power *absorption* coefficient (α) by

$$\alpha = 2\pi\bar{\nu}\varepsilon''/n \tag{5}$$

with

$$n = \{\tfrac{1}{2}[(\varepsilon'^2+\varepsilon''^2)^{\frac{1}{2}}+\varepsilon']\}^{\frac{1}{2}}.$$

It remains now to model ε^* with a statistical dynamical mechanism designed to reproduce the experimentally known ε^* features in dipolar liquids using a few equilibrium averages. The shape and frequency dependence of r_π and r_σ for various ϕ may then be calculated and evaluated.

MOLECULAR DYNAMICAL MODELS

It is advantageous to use molecular dynamical models to illustrate various aspects of reflection spectroscopy in the virtual total absence of the required reflection data at far-infrared frequencies for intensely absorbing liquids at incident angles away from the normal. The more sophisticated of these can be relied upon to describe satisfactorily the major features of absorption spectra and therefore serve as indicators.

We have used two recent models, that of Lobo *et al.*[5, 6] and that of Evans *et al.*,[4] both with inertial and memory effects inbuilt. It is shown elsewhere [8] that the former corresponds to the latter with internal field considerations added. These do not produce spectral features not already present in the version by Evans *et al.* We remark in passing that this means that the features labelled by Lobo *et al.* and Ascarelli [9] as " plasmons " can be described by autocorrelation functions and cannot be attributed to collective electrodynamic oscillations.

In the following section we calculate reflection spectra from model fittings of known absorption spectra in the far infrared. The parameters $K_0(0)$, $K_1(0)$ and γ used in these fittings are explained fully in the literature.[5, 10] We present some illustrative spectra and discuss the relative merits of power absorption and reflection spectroscopy.

ILLUSTRATIONS OF r_π AND r_σ

The spectra are conveniently presented as $\log_{10}\omega$ against $-\ln R$, (or against R) in fig. 1-14 for various K_0, K_1 and γ. The possibility of varying ϕ in the experimental set-up and using π and σ polarisation widens the range of data attainable in terms of number of spectral parameters. By using the same spectrometer, therefore, a much

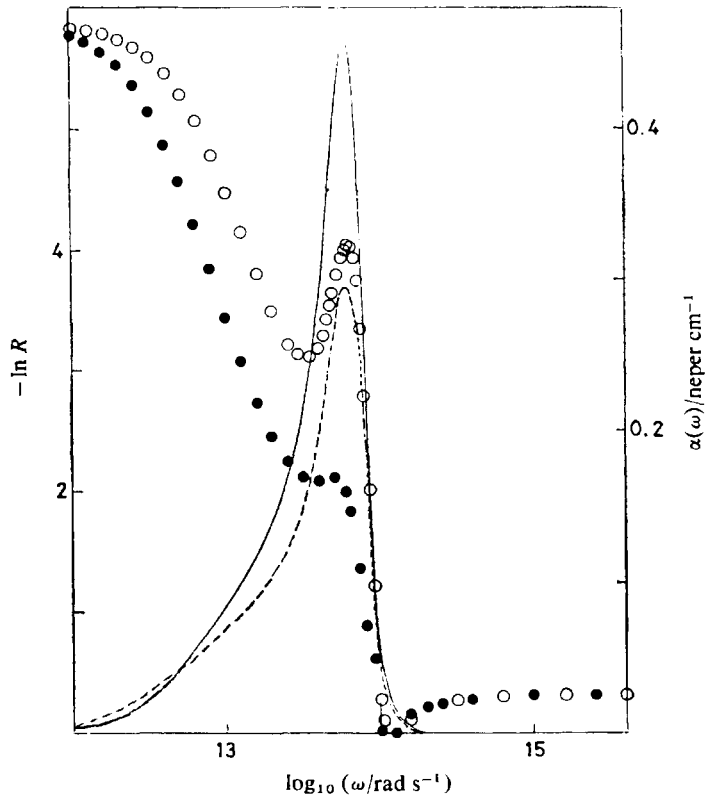

FIG. 1.—Theoretical absorption and reflection for liquid HCl (——) power absorption coefficient, $\alpha(\omega)$, Evans three variable theory [10] (see table 1). (- - -) The same for the theory of Lobo *et al.*[5] Power reflection coefficient, R at normal incidence ($\phi = 0$): ○, Evans theory; ●, Lobo *et al.* $\varepsilon_0 = 28.6$, $\varepsilon_p = 1.89$.

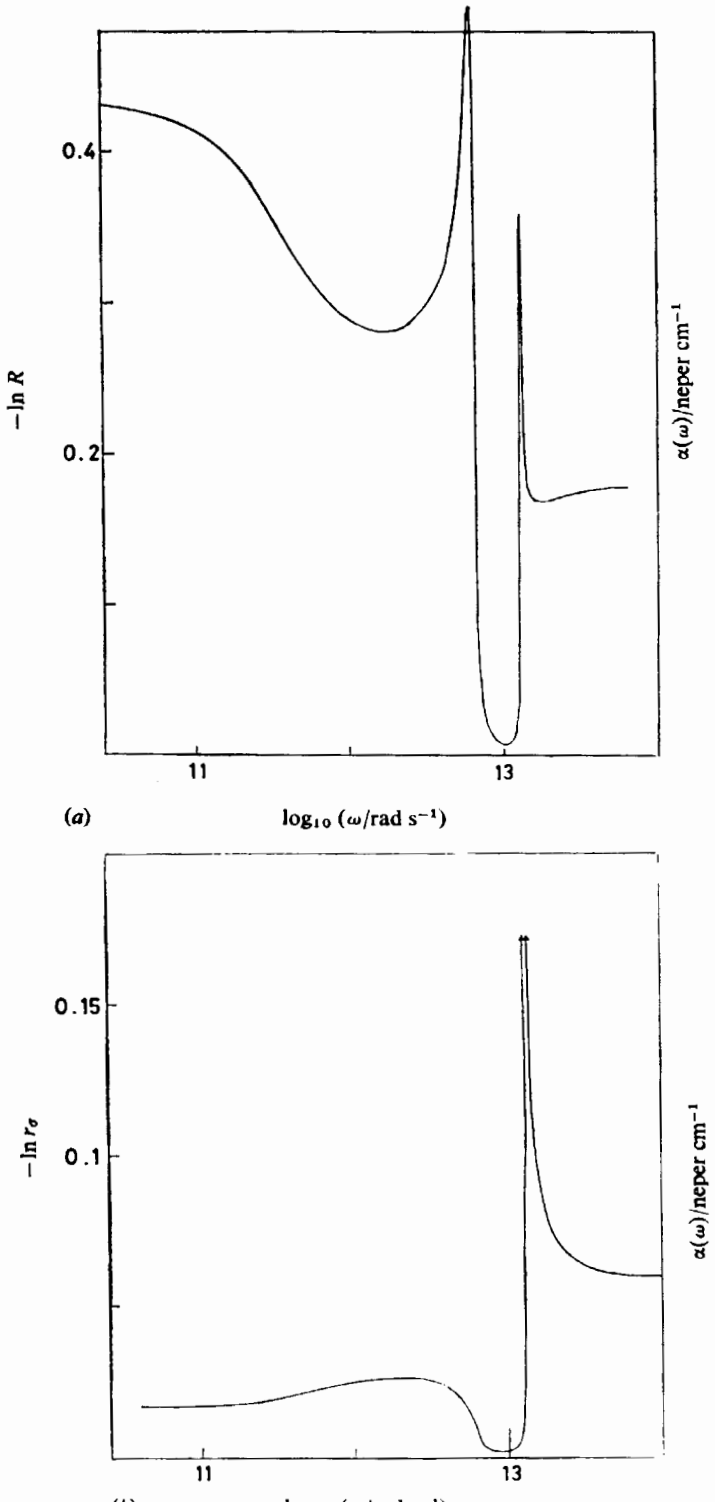

FIG. 2.—(*a*) Nitromethane liquid, $-\ln R$ from Evans three variable theory, $R = r_\pi$ polarisation (see text). Reflection at a glancing angle of $\phi = 1.55$ rad. Parameters quoted by Ascarelli.[9] $\varepsilon_0 = 25$; $\varepsilon_p = 3$. (*b*) $-\ln r_\sigma$ against $\log_{10} \omega$.

more rigorous testing of analytical theories is possible in using both reflection and absorption techniques. Reflection spectroscopy also has practical advantages when dealing with intense absorbers, such as biological material or semiconductors.

Fig. 1 illustrates r_σ and r_π at normal incidence for the very intensely absorbing liquid HCl, with the tabulated values of K_0, K_1 and γ used by Lobo *et al.* At normal incidence ($\phi = 0$) the R and α features (the Poley absorption) peak at the same frequency. The low frequency shoulder in α, accentuated in R ($= r_\pi = r_\sigma$ for $\phi = 0$), being the Debye loss peak in ε'', or loss representation. The effect of the internal field correction is to decrease the intensity, but not to introduce any extra spectral feature. This is always true for all values of ϕ, K_0, K_1 and γ in fig. 1-14.

The features labelled as " plasmons " by Lobo *et al.* and Ascarelli [9] may easily be reproduced in r_π and r_σ without any internal field (fig. 2), with a glancing angle of of $\phi = 1.55$ rad. These, unfortunately, have little or no physical significance since the values of K_0, K_1 and γ chosen for reflectivity data by Ascarelli [9] (table 1) do not correctly reproduce the observed α and ε'' features (fig. 3). Similarly, the values chosen by Lobo *et al.* for water (see table 1) are unrealistic, especially the case $\tau_0/\tau = 1$, which emphasised the " plasmon " peaks.

In what follows we have therefore taken the K_0, K_1 and γ values used by Evans and Evans [10] to describe ε'' and α in various dipolar liquids and also the nematic mesophase of *p*-dimethoxybenzylidene *p'*-n-butylaniline (MBBA) as bases for the

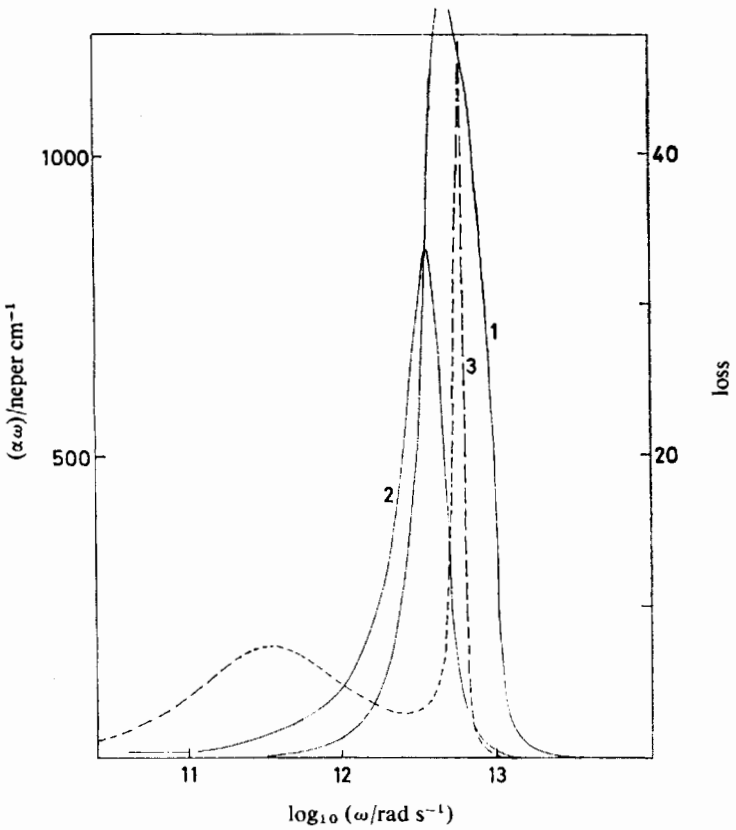

FIG. 3.—Nitromethane liquid, $\alpha(\omega)$ and dielectric loss $\varepsilon''(\omega)$ for the Ascarelli parameters. (1) $\alpha(\omega), \gamma = 10^{13}\ s^{-1}$; (2) $\varepsilon''(\omega), \gamma = 10^{13}\ s^{-1}$; (3) $\varepsilon''(\omega), \gamma = 10^{12}\ s^{-1}$.

TABLE 1.—PARAMETERS K_0, K_1 AND γ USED IN FIG. 1-14

fig.	$K_0(0)$ /10^{24} s^{-1}	$K_1(0)$ /10^{24} s^{-2}	$\gamma/10^{24}$ s^{-1}
1	313.8	313.8	45.5
2	11.8	29.5	1
3	11.8	29.5	1 and 10
4-8	1.43	15.0	6.0
9, 10	8.96	296.0	14.7
11	11.8	29.5	1
12	313.8	313.8	45.5
13, 14	1.12	288.0	2.4

calculation of r_σ and r_π. (In the meantime this work has been greatly extended by Reid [11] to many hundreds of other specimens and has been reviewed.[1]) A set of r_σ and r_π curves for tabulated (K_0, K_1, γ) is illustrated in fig. 4-7 for various angles ϕ. The set of (K_0, K_1, γ) used represents " large angled jump " motion such as that in a pseudo-spherical molecule in a relatively low-density liquid environment (or a highly compressed gas, but reflection is of course ruled out in this case experimentally). The features in r_π and r_σ are different for different ϕ, which is in itself very useful, but near the Brewster angle, $\phi_B = \tan^{-1} \varepsilon_p^{\frac{1}{2}}$, (fig. 8), and for a few degrees either side of ϕ_B, the behaviour of r_π becomes more interesting, in that an extra peak appears theoretically in the mid-infrared which could be used experimentally to investigate the molecular dynamics in a novel manner. Also, for the first time we see in this mid-infrared peak a fair difference between the ε'' peaks, but not in the α peaks (but

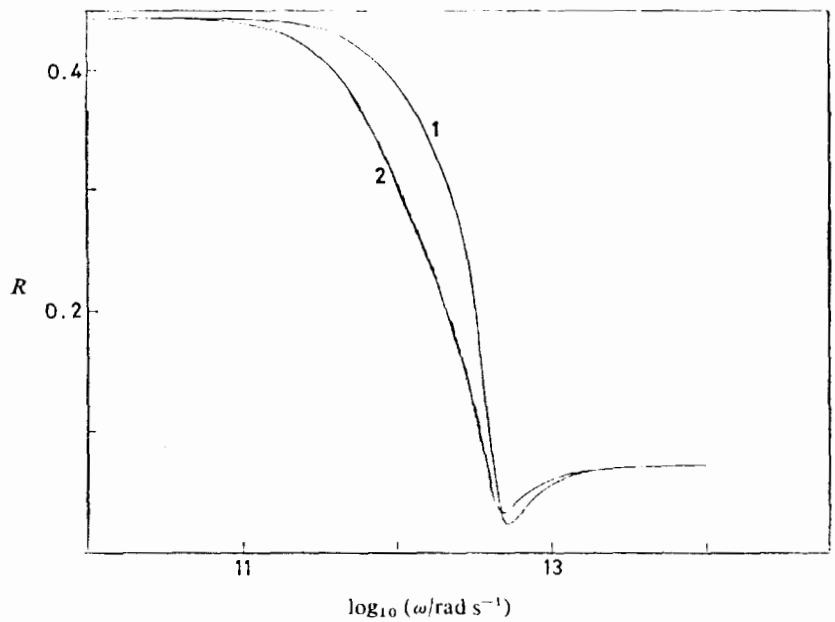

FIG. 4.—R plotted against log ω for a dynamical model of " large angled jumps ", parameters tabulated: $\phi = 0$, (——) Evans three variable; (- - -) Lobo *et al.* $\varepsilon_0 = 25$; $\varepsilon_p = 3$.

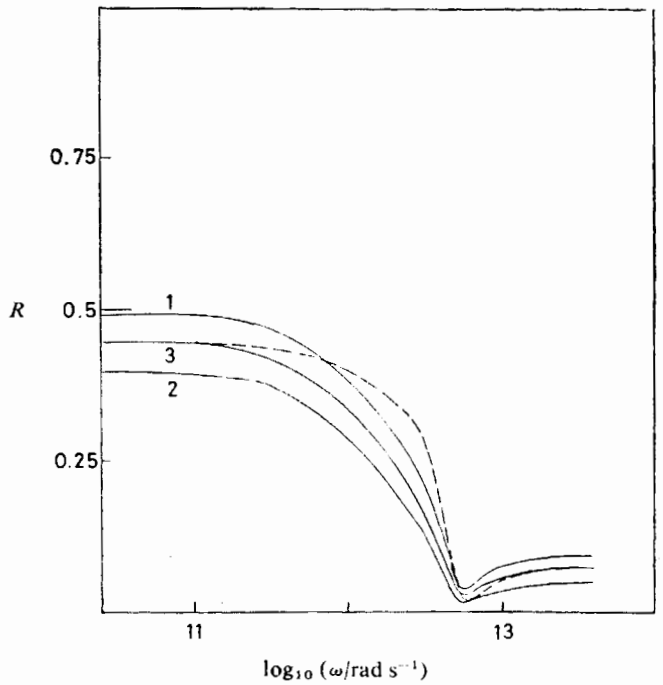

FIG. 5.—As for fig. 4; ϕ = 0.5 rad (28.648°). (——) Lobo *et al.*; (1) r_σ; (2) r_π; (3) average. (- - -) Evans three variable, average.

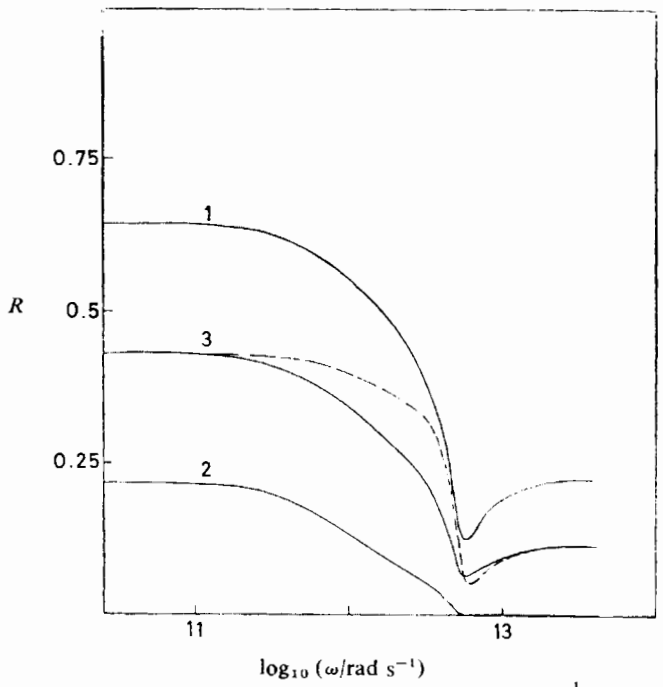

FIG. 6.—As for fig. 5; ϕ = 1.0 rad (57.296°); Brewster angle $\tan^{-1} \varepsilon_p^{\frac{1}{2}}$ = 1.047 rad (60.000°).

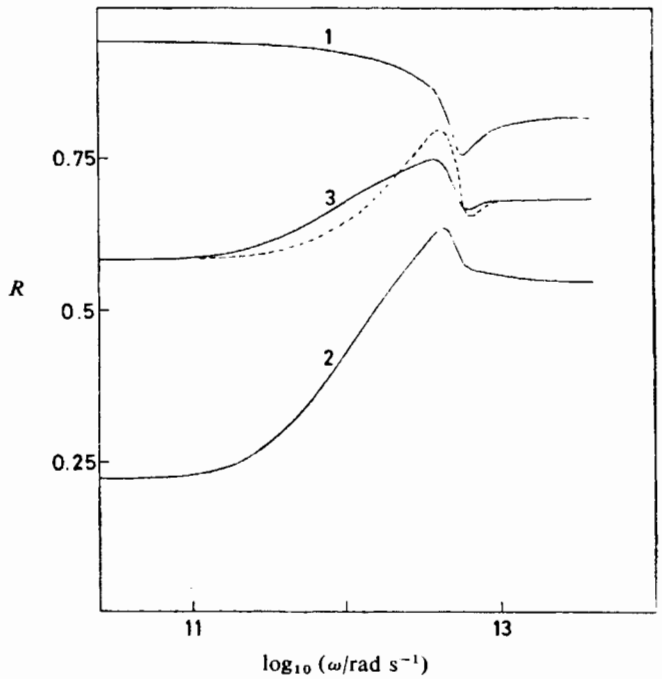

FIG. 7.—As for fig. 5; $\phi = 1.5$ rad (glancing angle).

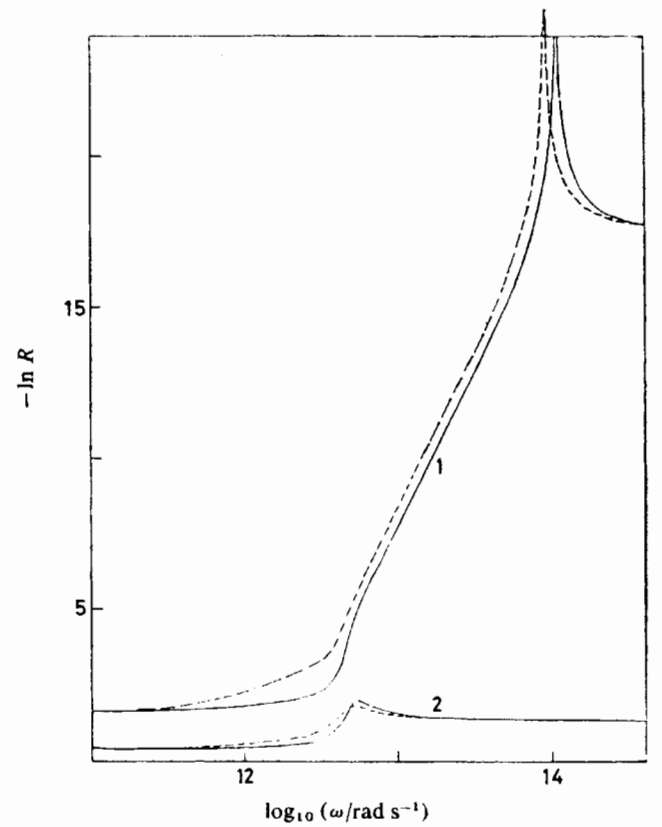

FIG. 8.—As for fig. 5; $\phi = 1.047$ rad $= \tan^{-1} e_p^{\frac{1}{2}}$, plot of $-\ln R$ against $\log_{10} \omega$. (1) r_π (——) Evans three variable, (- - -) Lobo *et al.* (2) r_σ.

we are not directly concerned with absorption spectroscopy here). This mid-infrared peak has not yet been investigated experimentally. The problem of heavy attenuation (*e.g.*, $\ln r_\pi = -20$) could be eased considerably and the noise level could be kept manageable by using intense laser radiation and an incidence angle ϕ close to but not at ϕ_B. Strictly speaking ε_p is still varying slightly at the upper frequency end of the Poley absorption (the α peak) so that ϕ_B cannot be defined probably better than a few tens of minutes of arc. Measurements with ϕ within a few degrees of this value should produce the mid-infrared feature in r_π. Note (fig. 8) that the r_σ value calculated from both models shows no such feature but retains the peak in the far-infrared (corresponding to α) and the lower frequency shoulder corresponding to the absorption peak in ε'' at anything from the audio to mircowave range. The far-infrared feature of r_σ is also retained in r_π.

A projected experimental set-up would involve an Apollo Instruments far-infrared laser system, tunable over 1500 lines producing monochromatic, polarised radiation a million times more intense than that available from a conventional black-body source (HP-16 high pressure mercury arc).

The same process is illustrated for a 4 % w/w solution of CH_3CN in CCl_4 in fig. 9 and 10. The absorption curves (ε'' and α) produced by the tabulated (K_0, K_1, γ) are illustrated with the experimental absorption data elsewhere.[12] The theoretical

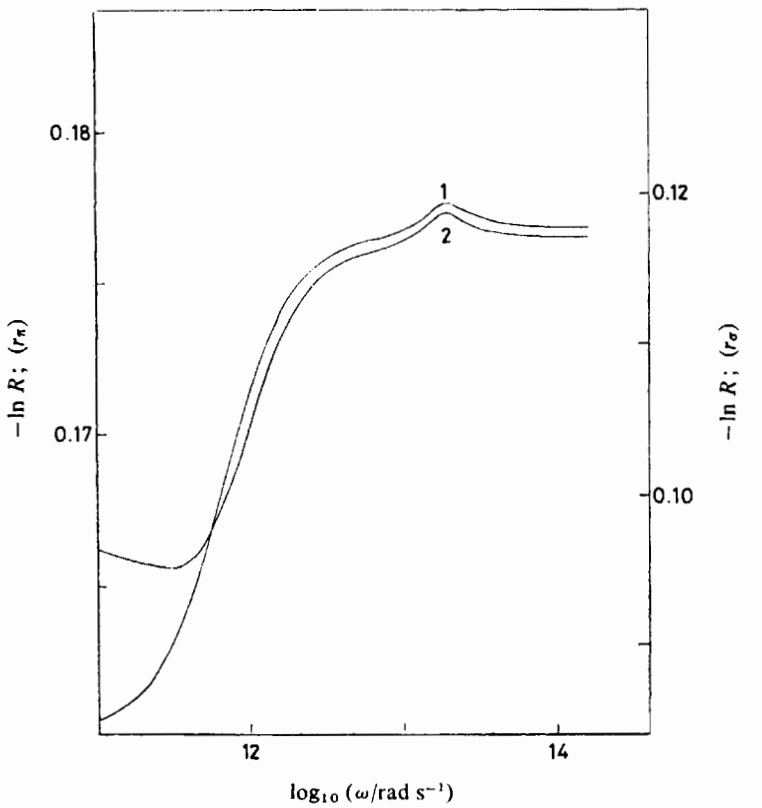

FIG. 9.—As for fig. 8, 4 % w/w solution of CH_3CN in CCl_4, best fit of three variable theory to α and ε''. Lobo *et al.* results give curves indistinguishable on this scale $\varepsilon_0 = 1.97$; $\varepsilon_p = 1.50$; $\phi = 1.55$ rad. (1) r.h. ordinate scale: r_σ, (2) l.h. ordinate scale: r_π.

curves are such that the shoulder and peak observable in fig. 9 are a little too accentuated, but are otherwise a fairly good representation of the measured data. In such a dilute solution the dynamical internal field is negligible, and both models give identical results on the scale of fig. 9 and 10. At a glancing angle of $\phi = 1.55$ rad the reflection spectrum is already interesting since the features in r_σ and r_π fall within the range of Michelson interferometry, which could therefore be used straightforwardly to measure the real and complex parts of n^* simultaneously. This has been exploited for normal incidence by Birch [13] and by Davies [14] but not yet for $\phi \neq 0$. Near ϕ_B ($= \tan^{-1} 1.50^{\ddagger}$, fig. 10), the r_π spectrum is dramatically different, one model being just distinguishable from the other by virtue of the mid-infrared peak in $-\ln r_\pi$ at over 600 cm^{-1}, within range of everyday grating instruments.

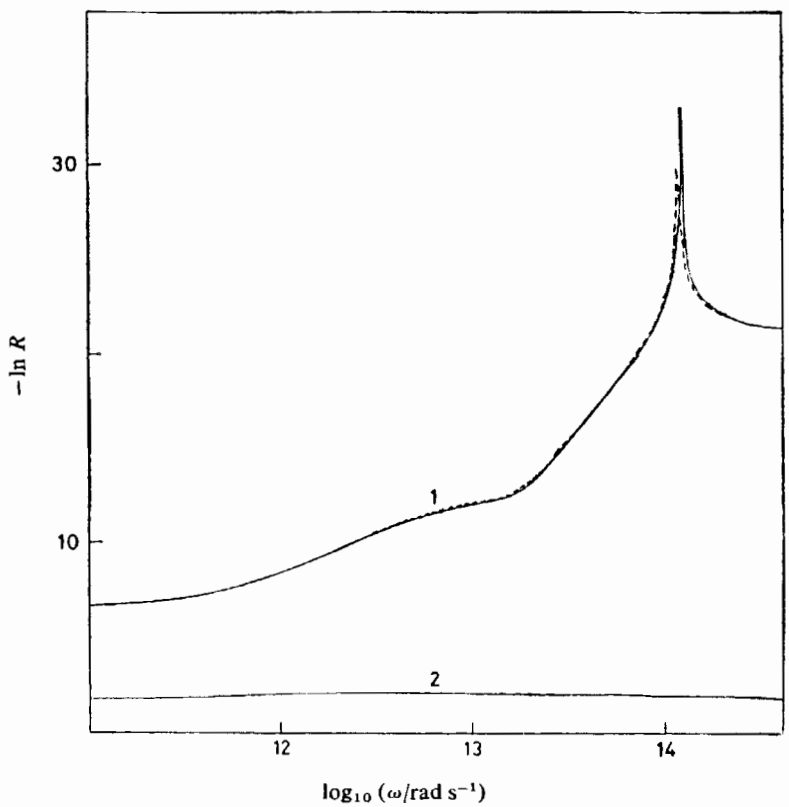

FIG. 10.—As for fig. 9; $\phi = \tan^{-1} \varepsilon_p^{\ddagger}$; (1) r_π; (——) Evans 3 variables; (- - -) Lobo *et al.* (2) r_σ; both theories; $\varepsilon_0 = 2.79$; $\varepsilon_p = 2.19$.

With the (albeit unrealistic) values of (K_0, K_1, γ) used by Ascarelli for nitromethane the Brewster peak in r_π appears theoretically at 1602 cm^{-1} (fig. 11), and with the (equally unrealistic) set used by Lobo *et al.* for HCl, at over 3000 cm^{-1} (fig. 12) into the near infrared. The true position of these peaks could be found by using the measured far-infrared/microwave values of α, ε'', ε' and n, and inserting into the fundamental reflectivity equations for r_π near the Brewster angle defined by $\tan^{-1} n$ just above the Poley band in α.

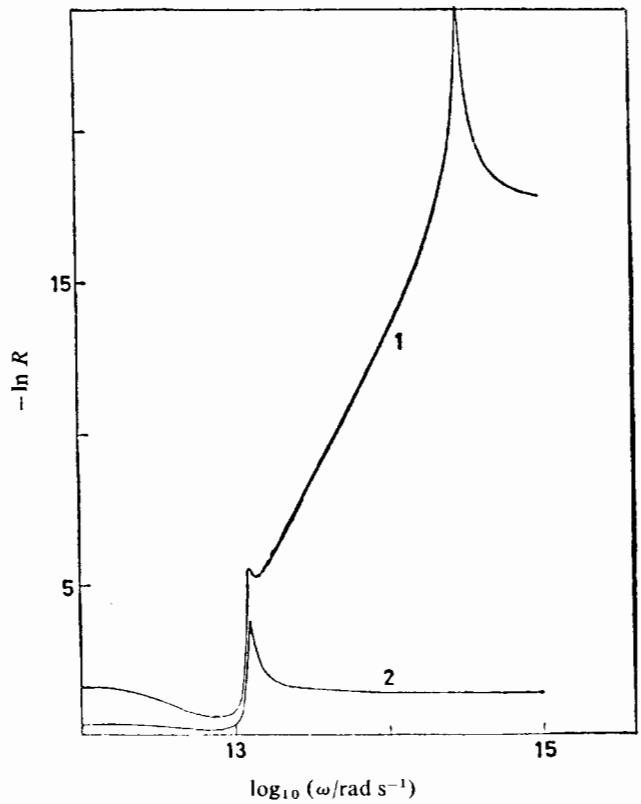

FIG. 11.—Plot of $-\ln R$ against $\log_{10}\omega$ for liquid nitromethane at $\phi = \tan^{-1}\varepsilon_p^{\frac{1}{2}}$. (1) r_π; (2) r_σ; Evans 3 variable theory.

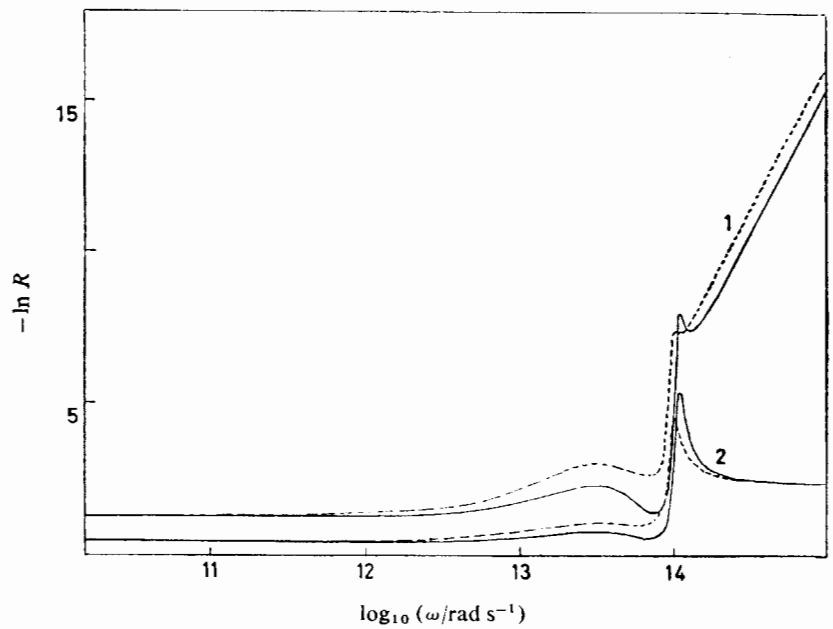

FIG. 12.—As for fig. 11; liquid HCl. (1) r_π (——) Evans 3 variable. (- - -) Lobo *et al.* (2) r_σ.

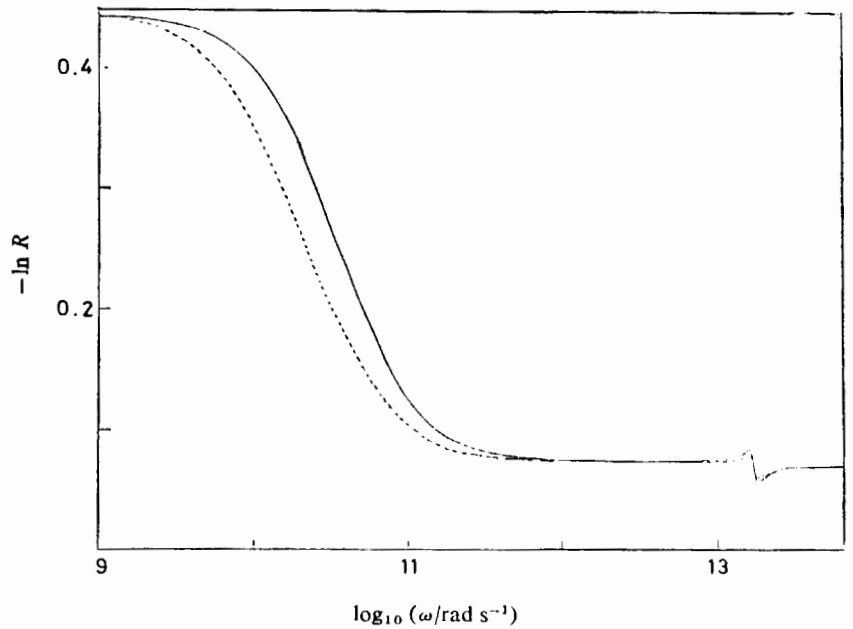

FIG. 13.—Plot of $-\ln R$ against $\log_{10}\omega$, isotropic MBBA, theoretical best fit. $\phi = 0$; $\varepsilon_0 = 25$; $\varepsilon_p = 3$ as test parameters. (——) Three variable theory. (- - -) Lobo *et al.*.

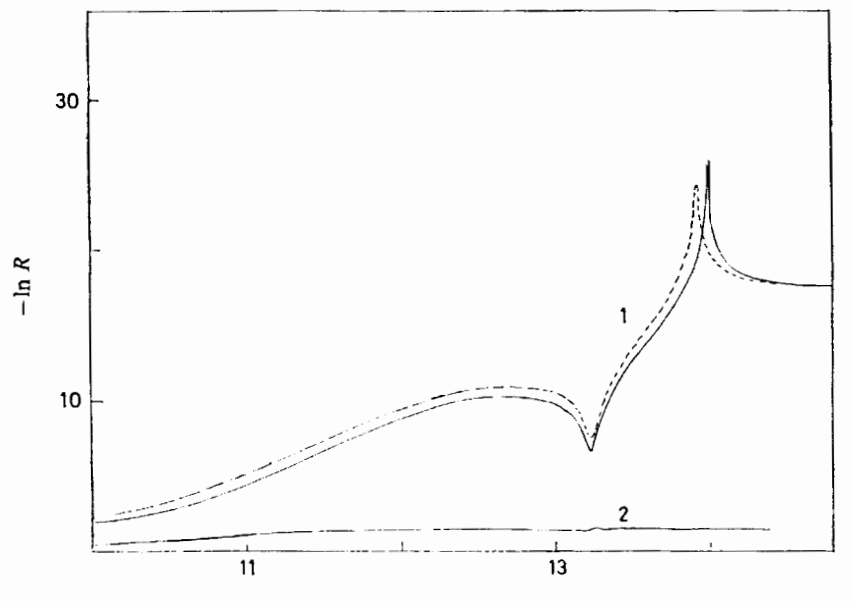

FIG. 14.—As for fig. 13, $\phi = \tan^{-1}\varepsilon_p^{\frac{1}{2}}$ (60.000°); plot of $-\ln R$ against $\log_{10}\omega$. (1) r_π; (——) Evans three variable; (- - -) Lobo *et al.* (2) r_σ; theories indistinguishable on this scale.

The true power of Brewster angle reflection spectroscopy may be illustrated by reference to fig. 13 and 14, where the (K_0, K_1, γ) parameters are those used by Evans and Evans [10] for the isotropic and nematic phases of MBBA. At normal incidence the reflection spectrum is featureless except for an inflection at $\log_{10}\omega = 13.2$. Near the Brewster angle, however, (fig. 14) a secondary peak in r_π appears at 484 cm^{-1}, which is shifted away from the value derived from the model of Lobo *et al.* The features in the far-infrared are considerably modified and r_σ retains the same overall form. Given sufficient amplification, therefore, reflection spectroscopy will be rewarding for this relatively heavy absorber.

DISCUSSION

In this section we summarise the implication of using power reflection far- and mid-infrared spectroscopy to study the molecular motions in bulk dipolar liquids and surfaces of any kind which are properly prepared.

(i) The variation of incident angle ϕ produces a variety of spectral bandshapes which can be used to complement absorption spectroscopy of heavily attenuating fluids and solids.

(ii) Near the Brewster incident angle, $\phi_B = \tan^{-1}\varepsilon_p^{\frac{1}{2}}$, there appear in r_π extra features in the mid- and near-infrared region which bring the study of the Poley/Debye process within range of tunable infrared lasers and grating spectrometers, provided the amplification system is sensitive enough to overcome the heavy attenuation.

(iii) The two models of molecular motion used to produce (i) and (ii) are versions of the same theory with and without internal field corrections and there are no features in one which are not present in the other. The split seen by Ascarelli in the glancing spectrum of nitromethane cannot therefore be explained in terms of collective hydrodynamic plasmons but is merely a natural consequence of the fundamental equations of reflection spectroscopy. The Evans three variable theory [10] contains no electrodynamic field corrections yet reproduces all the features inherent in the Lobo theory.[5] Therefore it follows that there are no plasmons, since the former theory is strictly one of autocorrelations alone. Ascarelli used a glancing angle ϕ to pick up an assumed coupling between the reflected electromagnetic wave and longitudinal " plasmon ". By reference to fig. 1-14, however, it can be seen by direct calculation that there is no special structure at the glancing angle which is not there near the normal angle. The really interesting region for r_π is that around the Brewster angle.

(iv) The concept of Brewster angle reflection spectroscopy is not limited to the far-infrared and lower frequency but could be applied to interferometry to shift structure normally seen in the mid-infrared up to visible frequencies, and so on. The study of gas–solid surface variations and the other phenomena of surface science in this way could be useful, always providing that the attenuation problems could be handled with sufficiently sensitive amplifiers and detectors. Probably the most useful feature of Brewster angle reflection spectroscopy is that of shifting structure away from the " difficult " far-infrared region into the mid-infrared and near-infrared.

I thank S.R.C. for extensive financial support and Dr. G. J. Evans for valuable discussions.

[1] M. W. Evans, G. J. Evans and A. R. Davies, *Adv. Chem. Phys.*, 1980, **44**, in press.
[2] W. Brugel, *An Introduction to Infra-red Spectroscopy* (Methuen, London, 1962), p. 332.
[3] G. W. Chantry, *Submillimetre Spectroscopy* (Academic Press, London, 1971).

[4] M. W. Evans, *Dielectric and Related Molecular Processes* (Spec. Period. Rep., The Chemical Society, London, 1977), vol. 3, p. 1.
[5] R. Lobo, J. E. Robinson and J. Rodriguez, *J. Chem. Phys.*, 1973, **59**, 5992.
[6] T. W. Nee and R. Zwanzig, *J. Chem. Phys.*, 1970, **52**, 6353.
[7] *Complex Permittivity*, ed. B. K. P. Scaife (English Univ. Press, London, 1971).
[8] M. W. Evans and G. J. Evans, *J.C.S. Faraday II*, in press.
[9] G. Ascarelli, *Chem. Phys. Letters*, 1976, **39**, 46.
[10] G. J. Evans and M. W. Evans, *J.C.S. Faraday II*, 1975, **73**, 1051.
[11] C. J. Reid and M. W. Evans, *J.C.S. Faraday II*, in press.
[12] M. W. Evans, G. J. Evans, J. Yarwood, P. L. James and R. Arndt, *Mol. Phys.*, 1979, **38**, 699.
[13] J. Birch, N.P.L. internal report.
[14] G. J. Davies, Post Office internal report.

(PAPER 9/1450)